

Crystallographic phase composition and structural analysis of Ti-Ni-Fe shape memory alloy by synchrotron diffraction

H. Sitepu^{1,2,a}, H.-G. Brokmeier^{3,b} and D. Chateigner^{4,c} and J.P. Wright^{5,d}

¹Institut Laue-Langevin (ILL), BP 156, 38042 Grenoble Cedex 9, France

²Present address: The University of British Columbia, reside at SRC, 15 Innovation Blvd.,
Saskatoon, SK, Canada, S7N 2X8.

³GKSS-Research Center, Max-Planck-Str., D-21502 Geesthacht, Germany

⁴CRISMAT-ISMRA, UMR CNRS n° 6508, Bd. Maréchal Juin, 14050 Caen, France

⁵ESR, BP 220, 38043 Grenoble Cedex, France

^asitepu@scr.sk.ca, ^bHeinz-gunther.Brokmeier@gkss.de,

^cDaniel.Chateigner@ismra.fr, ^dwright@esrf.fr

Keywords: Synchrotron high resolution powder diffraction (SRD); Trigonal R-phase martensite; Monoclinic (B19') martensite; Rietveld refinement; Generalized spherical harmonic (GSH) description.

Abstract: The preferred crystallographic orientation (*i.e.* texture) and the non-transformed austenite can cause serious systematic errors in the structural study of the R-phase in 50.75at.%Ti-47.75at.%Ni-1.50at.%Fe (hereafter referred to as Ti-Ni-Fe ternary) shape memory alloy. The crystal structure refinement of R-phase synchrotron high resolution powder diffraction (SRD) data using Rietveld refinement with generalized spherical harmonic (GSH) description for preferred orientation correction showed that the sample consists of minor cubic phase and the space group was $P\bar{3}$ [1]. The objective of the present paper is to study the crystallographic phase composition and crystal structure refinement of SRD data of trigonal R-phase martensite and monoclinic (B19') martensite in Ti-Ni-Fe ternary alloy during thermal cycling using the GSH description.

Introduction

The trigonal R-phase martensite transformation in Ti-Ni-Fe ternary shape memory alloy (SMA) has been widely used in the fundamental research because of the shape memory effect (or superelasticity). Also, the R-phase transformation has small thermal hysteresis which is very useful for actuators applications [2]. In order to understand the mechanism of the transformation, it is necessary to know the crystal structures of the R-phase and B19'-phase during thermal cycling. Using Rietveld refinement with random orientation of the crystallites, Hara *et al.* [3,4 and references therein] showed that the space group of the polycrystalline Ti-Ni-Fe R-phase X-ray powder diffraction (XRD) data at room temperature was $P\bar{3}$. They indicated that the rod shaped Ti-Ni-Fe alloy has the fiber texture with $\langle 111 \rangle$ of the parent cubic phase which had not been corrected. Therefore, the precision of the results [3,4] needs further special attention because texture can cause serious systematic errors in quantitative phase analysis and structure refinement from powder diffraction data [5].

Subsequently, the crystal structure of the rod shaped Ti-Ni-Fe alloy was non-destructively determined by Sitepu [1] using SRD data. The results obtained from Rietveld refinement with the GSH description [6-9] for preferred orientation correction [5] of all R-phase SRD data sets (*e.g.* from (303±7)K to (283±7)K, on cooling) indicated that:

- (i) for texture in SRD data sets of R-phase the reasonable crystal structure parameters was obtained when applying correction to intensities using the GSH description,
- (ii) the weight percentage of the non-transformed austenite was approximately 3%, and

- (iii) no significant improvement in goodness-of-fit index was found (see Fig. 1) when the inversion center was removed from the $P\bar{3}$ model, suggesting that the space group was indeed $P\bar{3}$ and not $P3$.

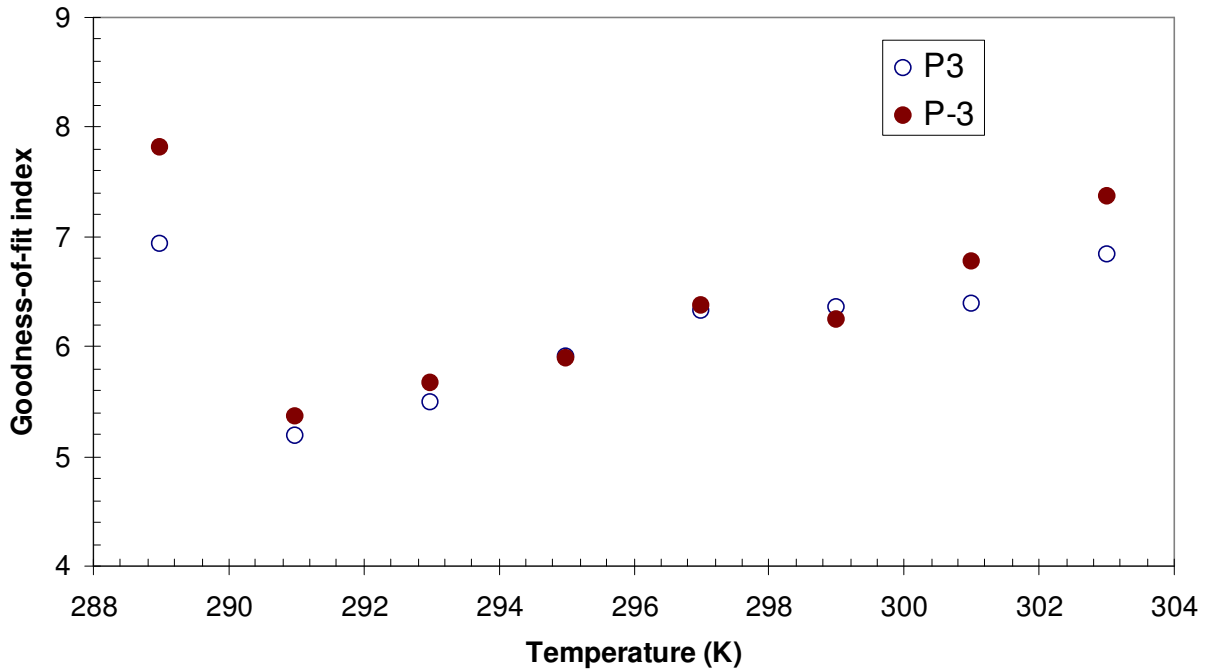


Fig. 1. Variation in crystallographic goodness-of-fit index (χ^2) with temperature for the R-phase martensite in Ti-Ni-Fe SMA when the GSH description was used in the refinement. The χ^2 values for $P3$ space group provided quite similar results than that for $P\bar{3}$ space group even though the number of atom positions refined in the $P\bar{3}$ was 0.5 times smaller than that of the $P3$ [1]. Also, the $R(F^2)$ factor reported by Hara *et al.* [2,3] from Rietveld refinement with random orientation for XRD data was 2.5 times higher than that of the corresponding $R(F^2)$ value determined by Sitepu [1] using the GSH description for SRD data.

The objective of the present study was to use the synchrotron X-ray high resolution powder diffractometer for describing the crystallographic phase composition and structural refinement of the rod shaped Ti-Ni-Fe ternary alloy during thermal cycling. The chief virtue of the synchrotron source is the combination of substantial penetration with high intensity and high spatial and angular resolution, which gives fast data acquisition rates. The GSH formulation was used to analyze SRD for the cubic, R-phase and monoclinic phases. This study yields very accurate crystal structure parameters for both R-phase and B19'-phase which to the best of our knowledge there have been no detailed analysis published simultaneously in the literature.

Experimental

Specimen

The rod shaped Ti-Ni-Fe ternary alloy with a diameter of 10 mm and 30 mm height, which has a $\langle 111 \rangle_{b_2}$ fiber texture, was provided by Professor Takuya OHBA of Shimane University in Japan. It was reported by Hara *et al.* [3,4] that the specimen was heat-treated at 1273 K and provided the Martensite starting (M_s) and finishing (M_f) transformation temperatures at (i) 310 K and 299 K for trigonal and (ii) 284 K and 248 K for monoclinic (B19'), see Figure 3 of Sitepu [1].

Data collection

The ID31 high resolution powder diffractometer at the ESRF in Grenoble, France with the energy of 60 keV ($\lambda = 0.2069 \text{ \AA}$) was used to measure SRD data of the rod shaped Ti-Ni-Fe. After mounting the alloy in the ID31 diffractometer it was heated up to $(373 \pm 7) \text{ K}$ where it was held for 360 s to reach thermal equilibrium. The temperature was then slowly cooled down to $(333 \pm 7) \text{ K}$ and also held for 360 s. Then the first SRD was measured for 6 hours. After that the temperature was slowly cooled down to $(297 \pm 7) \text{ K}$ where it was also held for 360 s. The second data was measured for 6 hours. The alloy was spun during the data collection to improve the particle statistics. It is noted, though, that the cylindrical symmetry on the texture is assured if the sample is spun during the data collection. The sample texture symmetry was chosen to be cylindrical in GSAS Rietveld refinement with GSH description (see below). Next, the temperature was slowly cooled down to $(268 \pm 7) \text{ K}$ where it was also held for 360 s to reach thermal equilibrium. Finally, the last data was collected for 6 hours. The 2θ scan range was three scans from 2° to 22° each at a slightly rock in phi with a 2θ step size of 0.008° . The data were then bin for each scan to yield a single histogram. Fig. 2 depicts the R-phase transformation in Ti-Ni-Fe using SRD data. As expected, the Ti-Ni-Fe shape memory effect is based on martensitic phase transitions from cubic (B2) austenitic phase at $(333 \pm 7) \text{ K}$ to trigonal R-phase martensite at $(297 \pm 7) \text{ K}$ and then gradually transformed to monoclinic (B19') martensite at $(268 \pm 7) \text{ K}$. Also, synchrotron X-ray beams provides very high intensity to background ratio. The ID31 instrument is described at the ESRF website, <http://www.esrf.fr>.

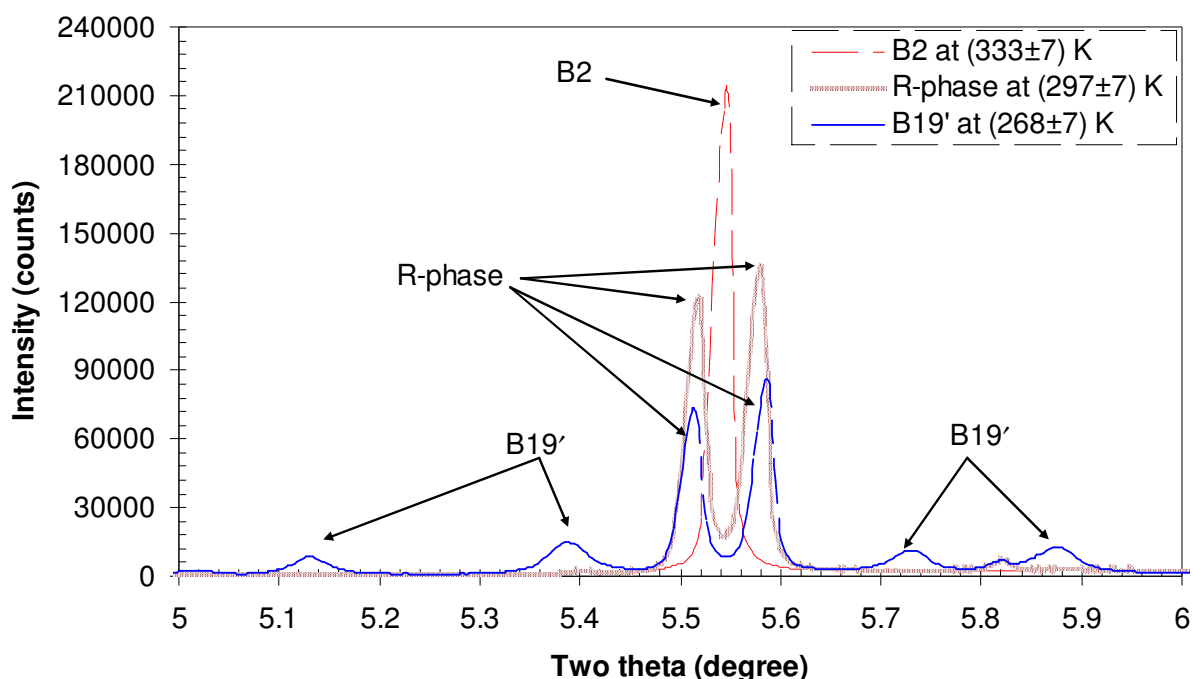


Fig. 2. Phase transformation of the rod shaped Ti-Ni-Fe ternary alloy SRD data, on cooling. As expected, the shape memory effect in Ti-Ni-Fe ternary alloy is based on martensitic phase transformations from the parent B2 cubic to the trigonal R-phase martensite and then the monoclinic (B19') martensite. The SRD data sets of the phases are consistent with the differential scanning calorimetry, on cooling curve.

Data Analysis

The B2, R-phase and B19' structural models used were described by Hara *et al.* [3,4], Sitepu [1] and Sitepu *et al.* [10], respectively. The Rietveld program used was GSAS [11] in which the GSH is

generated using selection rules depending on the crystal symmetry of the phase under investigation [6,7,8]. The refinement strategy was to release the phase scale factor (or phase abundance parameter) and the background component of the patterns with a 6-parameter Chebychev polynomial. The lattice parameters and zero point $2\theta_0$ (off-set in the 2θ scale of the goniometer) were released next followed by the Lorentzian and Gaussian terms of pseudo-Voigt profile function and anisotropic strain parameters [12,13]. Also, refined simultaneously with the structure were the crystal structure parameters, these included (a) the titanium [Ti₂(z), Ti₃(x), Ti₃(y), Ti₃(z)] and nickel [Ni₂(z), Ni₃(x), Ni₃(y), Ni₃(z)] coordinates for the R-phase and (b) the titanium [Ti(x) and Ti(y)] and nickel [Ni(x) and Ni(y)] for the B19' martensite as well as the full set of independent isotropic thermal parameters for all titanium and nickel atoms. Once the random orientation of the crystallites had converged, the GSH coefficients were then refined. The default sample texture symmetry was chosen to be cylindrical in the Rietveld refinement with the GSH description, and maximum eight harmonic orders was selected after preliminary calculations with ten orders gave the same results.

Results and Discussions

Summary of the results derived from Rietveld refinement with GSH description for SRD data set of Ti-Ni-Fe alloy during thermal cycling are given in Table 1. The values in parentheses are estimated standard deviations obtained from the Rietveld refinement. The R-phase and monoclinic B19'-phase martensite crystal structure parameters derived from the refinement agree quite satisfactorily with the results reported by Schryvers and Potapov [14] and Sitepu [1] for R-phase and Sitepu *et al.* [9, 10] for B19'. It is clearly seen from Table 1 that the R-phase cell parameters decrease slightly when the temperature decreases. While the isotropic temperature factors for all titanium atoms increases slightly, the corresponding temperature factors for all nickel atoms decreases gradually when the temperature increases. The atomic positions change decimally only as the temperature increases. The starting weight percentage of the R-phase at $(333\pm 7)\text{K}$ was 2.340(1) and increased dramatically when the temperature reached the R-phase transformation at $(297\pm 7)\text{K}$. Then, the corresponding weight percentage of the R-phase decreased dramatically from 97.085(7) to 34.879(1) as the temperature reduced to $(268\pm 7)\text{K}$. At this temperature, the weight percentage for the monoclinic (B19') was 65.121(1) which indicates that the R-phase has not fully transformed yet to B19'. It is interesting to note, that the B19' weight percentage were not appeared at above $(268\pm 7)\text{K}$. The weight percentages for B2, R-phase and B19' during thermal cycling are consistent with the differential thermal calorimetry curve, on cooling. Thus, the GSH description can be used to obtain the reasonable crystal structure parameters in the textured samples, but one must also determine the texture along with the structure. If the texture of the sample is important, it should be possible to refine the reasonable crystal structural parameters of a single SRD data set only if the texture can be approximated by a model with cylindrical symmetry with respect to the single SRD pattern. The cylindrical symmetry on the texture was assured if the sample spun during the data collection.

Table 2 shows the deviation of R-phase atomic co-ordinates from the positions in the parent B2 structure. Comparing with the original parent phase Ti(0,0,0) and Ni(0,0,0.5) positions, each third titanium (Ti) and nickel (Ni) plane in the R-phase separates into three layer with different z-coordinates. The deviations from the positions in the present B2 structure are 0.031c and 0.009c for the Ti₂ and Ti₃ atoms, respectively. The corresponding deviation values for the Ni₂ and Ni₃ atoms are 0.065c and 0.021c, respectively, which are two times bigger than that of the Ti₂ and Ti₃ atoms. However, the Ti₃ stay at approximately the same z-position as in the B2 parent phase in which the shift value is relatively very small.

Table 1. Refined crystal structure parameters for the cubic (B2) austenite, trigonal R-phase martensite and monoclinic (B19') martensite SRD data during thermal cycling

Parameters	Refined parameters	Atomic parameters derived from GSH description for SRD data a temperature of		
		(333±7)K	(297±7)K	(268±7)K
Space group		Pm3m	$P\bar{3}$	$P112_1/m$
<i>Cubic (B2) austenite</i>				
Cell parameter	a (Å) ²	3.0108(1)	3.005(2)	
Ti1(0, 0, 0)	100*Uiso (Å) ²	1.057(5)	1.057(5)	
Ni1(0, 0, 0.5)	100*Uiso (Å) ²	0.446(3)	0.446(3)	
<i>Trigonal R-phase</i>				
Cell parameters	a (Å) ²	7.3511(4)	7.3472(2)	7.3380(1)
	c (Å) ²	5.2784(3)	5.2837(3)	5.2918(3)
Ti1(0, 0, 0)	100*Uiso (Å) ²	1.049(20)	1.057(5)	1.647(7)
Ti2(1/3, 2/3, z)	z	0.030(1)	0.031(3)	0.030(1)
	100*Uiso (Å) ²	1.049(2)	1.057(5)	1.647(7)
Ti3(x, y, z)	x	0.333(1)	0.332(4)	0.330(03)
	y	-0.007(2)	-0.007(2)	-0.012(03)
	z	0.341(03)	0.342(2)	0.346(1)
	100*Uiso (Å) ²	1.049(2)	1.057(5)	1.647(7)
Ni1(0, 0, 1/2)	100*Uiso (Å) ²	0.548(6)	0.446(3)	0.025(4)
Ni2(1/3, 2/3, z)	z	0.560(1)	0.565(3)	0.573(1)
	100*Uiso (Å) ²	0.548(6)	0.446(3)	0.012(4)
Ni3(x, y, z)	x	0.322(04)	0.322(3)	0.320(02)
	y	-0.019(02)	-0.020(2)	-0.016(02)
	z	0.852(03)	0.854(2)	0.851(04)
	100*Uiso (Å) ²	0.548(6)	0.446(3)	0.012(4)
<i>Monoclinic (B19') phase</i>				
Cell parameters	a (Å) ²			2.8885(2)
	b (Å) ²			4.6304(3)
	c (Å) ²			4.1185(2)
	γ (°)			97.385(8)
Ti(x, y, 1/4)	x			0.583(1)
	y			0.287(03)
	100*Uiso (Å) ²			0.503(9)
Ni(x, y, 3/4)	x			0.026(1)
	y			0.174(03)
	100*Uiso (Å) ²			0.503(3)
<i>Weight percentage (wt%)</i>				
	B2	97.660(01)	2.915(3)	0.000
	R-phase	2.340(1)	97.085(7)	34.879(1)
	B19'	0.000	0.000	65.121(1)

Table 2. Deviation of the atomic co-ordinate for the trigonal R-phase martensite SRD data at (297±7)K from the positions in the parent cubic (B2) austenite structure

Parameters	Wyckoff code ¹	x	y	z	Deviation from the positions in the parent B2 structure		
					Δx	Δy	Δz
Ti1	1(a)	0	0	0	-	-	-
Ti2	2(d)	1/3	2/3	0.031(3)	-	-	0.031
Ti3	6(g)	0.332(4)	-0.007(2)	0.342(2)	-0.001	-0.007	0.009
Ni1	1(b)	0	0	1/2	-	-	-
Ni2	2(d)	1/3	2/3	0.565(3)	-	-	0.065
Ni3	6(g)	0.322(3)	-0.020(2)	0.854(2)	-0.011	-0.020	0.021

¹ Co-ordinates, 1(a) = 0, 0, 0; 1(b) = 0, 0, 1/2; 2(d) = 1/3, 2/3, z; 6(g) = x, y, z

Summary

Specific problems in the structural study of Ti-Ni-Fe ternary SMA are the preferred crystallographic orientation and the incomplete ordering from austenite to martensite. Therefore, the correcting of preferred orientation is of critical important in powder diffraction analysis for structural study and in the determination of bulk descriptors such as phase composition. The present study provides the reasonable crystal structure parameters for both R-phase and B19'. Also, the weight percentages for (a) the non-transformed austenite to R-phase at $(333\pm 7)\text{K}$ and (ii) R-phase to B19' at $(268\pm 7)\text{K}$ were given. The crystallographic structural refinement $R(F^2)$ figures-of-merit reported by Hara *et al.* [3,4] was $2.5\times$ higher than that of the corresponding value for SRD data. This clearly shows that the texture should be corrected in order to get accurate results. The weight percentage of the non-transformed austenite was 3 % which was not discovered by Hara *et al.* [3,4]. Moreover, the present results of B19' crystal structure parameters agree quite satisfactorily with the results reported by Sitepu *et al.* [10,11]. Therefore, it can be concluded that for texture in SRD data sets of R-phase and B19'-phase the accurate crystal structure parameters can be obtained when applying correction to intensities using the GSH description. Finally, the refinement results for all SRD data sets show that the phase composition during the martensitic transformation are consistent with the differential scanning calorimetry, on cooling curve.

Acknowledgements

Thanks to Professor Takuya Ohba for providing the Ti-Ni-Fe ternary alloy. Thanks to Dr F. Fauth for his help in conducting the experiment and interpreting the results. Thanks to Dr Alan W. Hewat for his help in conducting the early refinement with the center symmetry of the R-phase. Thanks to ESRF for providing the beam time on the ME306 project.

References

- [1] H. Sitepu: *Texture and Microstructures* Vol. 35 (2003), p. 185
- [2] K. Otsuka and C.M. Wayman: *Shape Memory Materials* (Cambridge University Press, Cambridge, 1998).
- [3] T. Hara, T. Ohba and K. Otsuka: *J. de Physique III* Vol. 5 (1995), p. 641
- [4] T. Hara, T. Ohba, E. Okunishi and K. Otsuka: *Mater. Trans. JIM* Vol. 38 (2007), p. 11
- [5] H. Sitepu: *J. Appl. Cryst.* Vol. 35 (2002) p. 274
- [6] H.J. Bunge: *Texture Analysis in Materials Science* (Butterworths, London 1982).
- [7] N.C. Popa: *J. Appl. Cryst.* Vol. 25 (1992), p. 611
- [8] R.B. Von Dreele: *J. Appl. Cryst.* Vol. 30 (1997) p. 517
- [9] H. Sitepu, W.W. Schmahl and R.B. Von Dreele: *Appl. Phys. A* Vol. 74 (2003), p. S1676
- [10] H. Sitepu, W.W. Schmahl and J.K. Stalick: *Appl. Phys. A* Vol. 74 (2003), p. S1919
- [11] A.C. Larson and R.B. Von Dreele: *General structure analysis system (GSAS)* (Los Alamos National Laboratory Report LAUR, 2000).
- [12] N.C. Popa: *J. Appl. Cryst.* Vol. 31 (1998), p. 176
- [13] P.W. Stephens: *J. Appl. Cryst.* Vol. 32 (1999), p. 281
- [14] D. Schryvers and P.L. Potapov: *Materials Trans.* Vol. 43 No. 5 (2002), p. 774